Cellular Physiology and Biochemistry

Cell Physiol Biochem 2015;35:1557-1570

DOI: 10.1159/000373971
Published online: March 12, 2015

Accepted: January 20, 2015

1421-9778/15/0354-1557$39.50/0

Original Paper

Emodin Protects Against Concanavalin A-Induced Hepatitis in Mice Through Inhibiting Activation of the p38 MAPK-NF-κB Signaling Pathway

Jihua Xue[a] Feng Chen[a] Jing Wang[a] Shanshan Wu[a] Min Zheng[a] Haihong Zhu[a] Yanning Liu[a] Jiliang He[b] Zhi Chen[a]

[a]State Key Lab of Diagnostic and Treatment of Infectious Diseases, Collaborative Innovation Center for Diagnosis and Treatment of Infectious Disease, 1st Affiliated Hospital of Medical School, Zhejiang University, Hangzhou, [b]Institutes of Environmental Medicine, School of Medicine, Zhejiang University, Hangzhou, China

Key Words
Emodin • Con A • Cytokines • Chemokines • p38 MAPK • NF-κB • Immune cells

Abstract
Background/Aims: To investigate the effects of emodin on concanavalin A (Con A)-induced hepatitis in mice and to elucidate its underlying molecular mechanisms. ***Methods:*** A fulminant hepatitis model was established successfully by the intravenous administration of Con A (20 mg/kg) to male Balb/c mice. Emodin was administered to the mice by gavage before and after Con A injection. The levels of pro-inflammatory cytokines and chemokines, numbers of $CD4^+$ and $F4/80^+$ cells infiltrated into the liver, and amounts of phosphorylated p38 MAPK and NF-κB in mouse livers and RAW264.7 and EL4 cells were measured. ***Results:*** Pretreatment with emodin significantly protected the animals from T cell-mediated hepatitis, as shown by the decreased elevations of serum alanine aminotransferase (ALT) and aspartate aminotransferase (AST), as well as reduced hepatic necrosis. In addition, emodin pretreatment markedly reduced the intrahepatic expression of pro-inflammatory cytokines and chemokines, including tumor necrosis factor (TNF)-α, interferon (IFN)-γ, interleukin (IL)-1β, IL-6, IL-12, inducible nitric oxide synthase (iNOS), integrin alpha M (ITGAM), chemokine (C-C motif) ligand 2 (CCL2), macrophage inflammatory protein 2 (MIP-2) and chemokine (CXC motif) receptor 2 (CXCR2). Furthermore, emodin pretreatment dramatically suppressed the numbers of $CD4^+$ and $F4/80^+$ cells infiltrating into the liver as well as the activation of p38 MAPK and NF-κB in Con A-treated mouse livers and RAW264.7 and EL4 cells. ***Conclusion:*** The results indicate that emodin pretreatment protects against Con A-induced liver injury in mice; these beneficial effects may occur partially through inhibition of both the infiltration of $CD4^+$ and $F4/80^+$ cells and the activation of the p38 MAPK-NF-κB pathway in $CD4^+$ T cells and macrophages.

F. Chen contributes to this work equally.

Zhi Chen, PhD, MD,

The First Affiliated Hospital of Zhejiang University, 79 Qingchun Road, Hangzhou, Zhejiang 310003 (China)
Tel. +86-571-87236579, Fax +86-571-87068731, E-Mail zju.zhichen@gmail.com

Introduction

Fulminant hepatitis is a devastating inflammatory disease of the liver that is widespread in China and mainly develops from chronic or acute hepatitis B virus (HBV) infection. HBV-related end-stage liver disease and hepatocellular carcinoma (HCC) are responsible for over 0.5-1 million deaths per year [1-4], while acute fulminant hepatitis B causes an additional 40,000 deaths each year [5]. Fulminant hepatitis usually begins with a sudden onset and progresses rapidly, leaving little time for effective treatment, and it is associated with a significant mortality rate. Therefore, it is crucial to develop strategies for its prevention.

T cell-mediated immune responses play important roles in the development and progression of autoimmune and viral hepatitis [6-8]. Concanavalin A (Con A)-induced hepatic injury is a well-characterized murine model of T cell-mediated hepatic damage with a pathophysiology similar to those of human viral and autoimmune hepatitis [9, 10]. This model has been widely used to study the etiopathogenesis, pathogenesis, and clinical treatment of immunological hepatitis in humans [11]. Activated $CD4^+$ T cells and Kupffer cells play key roles in hepatocyte damage in this model. These cells infiltrate into the liver parenchyma and induce the secretion of pro-inflammatory cytokines, such as tumor necrosis factor (TNF)-α, interferon (IFN)-γ, interleukin (IL)-1, IL-6 and IL-4 [12-14]. Alanine aminotransferase (ALT) and aspartate aminotransferase (AST) become elevated as a result of hepatocyte necrosis following the intravenous administration of Con A [15].

Emodin (1,3,8-trihydroxy-6-methyl-anthraquinone), which is an anthraquinone derivative from the Chinese herb Radix et Rhizoma Rhei, has been reported to possess a variety of biological properties, such as anti-inflammatory [16], anti-viral [17], anti-tumor [18], and anti-oxidant activities [19]. Emodin was found to inhibit inflammatory cytokine production in HMGB1-induced inflammatory responses *in vitro* and *in vivo* [20] and to suppress inflammatory responses in TNF-α-induced aortic smooth muscle cells [21]. Emodin also has a protective effect on cholestatic hepatitis [22]. However, little is known regarding its effects on fulminant hepatitis. In the present study, we assessed the effects of emodin on the prevention of liver injury by establishing a mouse model of fulminant hepatitis induced by the intravenous injection of Con A, and the underlying molecular mechanisms were also investigated.

Materials and Methods

Animals

Balb/c mice (6-8 weeks old, male) were obtained from the Experimental Animal Center of the Chinese Science Academy (Shanghai, China), and all mice were housed under pathogen-free conditions. All procedures were performed according to the guidelines for the Care and Use of Laboratory Animals and approved by the ethics committee of the Zhejiang University School of Medicine.

Dose-effect relationship of emodin

Mice were randomly divided into control (vehicle), emodin (50 mg/kg body weight), Con A (20 mg/kg body weight), and emodin plus Con A (20 mg/kg body weight Con A plus 1.5625 mg/kg, 3.125 mg/kg, 6.25 mg/kg, 12.5 mg/kg, 25 mg/kg, and 50 mg/kg body weight emodin, respectively) groups, and each group contained 5 mice. Con A and emodin (Sigma Chemical Co., St. Louis, MO, USA) were prepared with pyrogen-free saline and sodium carboxymethyl cellulose (CMC-Na; Sigma Chemical Co., St. Louis, MO, USA), respectively. Emodin was administered orally, and Con A was given through intravenous injection at 2 h after emodin administration. In place of emodin, CMC-Na was used in the Con A group, and saline (vehicle) was used in place of Con A in the emodin group, and the normal control mice were treated with a vehicle. The mice were sacrificed 10 h after Con A injection.

Time-effect relationship of emodin

Mice were randomly divided into control (vehicle), emodin (25 mg/kg body weight), Con A (20 mg/kg body weight), and emodin plus Con A (20 mg/kg body weight Con A plus 25 mg/kg body weight emodin) groups, and each group contained 5 mice. In the emodin plus Con A group, emodin was administered orally at 2 h before and 30 min, 60 min, 90 min, and 2 h after Con A exposure, respectively. In place of emodin, CMC-Na was used in the Con A group, and saline (vehicle) was used in place of Con A in the emodin group, and the normal control mice were treated with a vehicle. The mice were sacrificed 10 h after Con A injection.

Pathologic evaluation

Hepatic sections were obtained from the mice. The sections were fixed with 10% neutral-buffered formalin, embedded in paraffin and cut into 3-5 μm slices. After deparaffinization and rehydration, the slices were stained with hematoxylin and eosin (H&E staining). All specimens were histologically assessed by two experienced pathologists. Five visual fields (10× magnification) randomly selected from each section were used for the image analysis. The area of necrotic liver tissue was measured using the Image-Pro Plus 5.0 software (Media Cybernetics, Inc., Bethesda, MD, USA). The necrosis rate of the hepatocytes was calculated according to the necrotic areas divided by the liver area of the image.

Biochemical detection

The blood was collected from the retro-orbital sinus in mice following exposure to Con A and/or emodin. Levels of serum ALT and AST were measured using the Automatic Chemical Analyzer 7600-100 (Hitachi, Ltd., Tokyo, Japan).

RNA preparation and analysis

Total RNA was extracted from tissues using TRIzol reagent (Invitrogen Corp., Carlsbad, CA) following the manufacturer's instructions. For the analysis, the total RNA (1 μg) was reverse-transcribed using the PrimeScript™ RT Reagent Kit with the gDNA Eraser (Code no. RR047A, Takara). The gene expression analysis of the mouse livers was performed by qRT-PCR with SYBR Premix EX TaqTM II (Code no. RR820A, Takara) using the ABI PRISM 7900 sequence detector (Applied Biosystems, Foster City, CA, USA). The total amplification reaction volume of 20 μL contained 2× SYBR® Premix Ex Taq™ Ⅱ, 0.4 μmol/L primers, and 1 μL of template cDNA. Thermal cycling was carried out for 30 s at 95 °C, followed by 40 cycles of 5 s at 95 °C, and 30 s at 60 °C. Each PCR assay was performed in triplicate, and the changes in mRNA levels were normalized by the levels of the control gene mRNA (β-actin). The activation of cells was determined by measuring RNA of TNF-α in RAW264.7 cells and IL-2 in EL-4 cells, respectively. RAW264.7 cells (2×10^5/ml) or EL4 cells (2×10^6/ml) were treated with or without emodin for 2 h and then were stimulated by Con A. After 24 h incubation, cells were collected and relative quantitative real time PCR was performed. The primers purchased from Sangon Biotech (Shanghai) are listed in Table1.

Table 1. Primer sequences of the nine primer sets used for RT-PCR

Gene	Upstream primer	Downstream primer
IFN-γ	atggctgtttctggctgttact	aatgacgcttatgttgttgctg
TNF-α	ggcaggtctactttggagtcat	cagagtaaaggggtcagagtgg
IL-2	cattgacacttgtgctccttgt	tcctgtaattctccatcctgct
IL-1β	tgaaatgccacctttgacag	ccacagccacaatgagtgatac
iNOS	gagccacagtcctctttgcta	tgtcaccaccagcagtagttg
ITGAM	gaccttccatccttcaacactc	gctccactttggtctctgtctt
CCL2	cagcaggtgtcccaaagaag	tgtggaaaaggtagtggatgc
MIP2	atccagagcttgagtgtgacg	gttagccttgcctttgttcag
CXCR2	taacaatacatcccgtttgagg	agtgtgaacccgtagcagaac
β-actin	aacagtccgcctagaagcac	cgttgacatccgtaaagacc

Immunofluorescence assay

The paraffin-embedded liver sections from both the normal and Con A-treated mice were deparaffinized, rehydrated, and treated with an antigen-repairing solution for the immunohistochemistry analysis. Thereafter, the sections were incubated with a blocking solution (5% BSA in PBS), followed by incubation with fluorescein isothiocyanate (FITC)-conjugated F4/80 or phycoerythrin (PE)-conjugated CD4 antibodies (BD Biosciences, San Diego, CA, USA) overnight at 4 °C. After washing with PBS 3 times, the sections were covered with coverslips and observed using a confocal microscope (Olympus Inc., Center Valley, PA, USA). The numbers of positive cells in each section were counted in five randomly selected fields in each group, and the mean number of immunoreactive cells was calculated for each case. Five mice in each group were analyzed.

Cell Culture and cytotoxicity analysis

Murine macrophage-like RAW264.7 cells and EL4 murine T-lymphoma cells were obtained from the American Type Culture Collection (ATCC, Rockville, MD). RAW264.7 cells were pre-cultured in DMEM medium (Gibco BRI, Grand Island, NY) supplemented with 10% fetal bovine serum (FBS). EL4 cells were maintained in RPMI 1640 medium (Gibco BRI, Grand Island, NY) supplemented with 10% FBS, 2 mM glutamine, 100 μg/ml of penicillin and 100 μg/ml of streptomycin. Cells were pretreated with emodin for 2h and then were stimulated by Con A for 24 h.

The cytotoxicity of Con A and emodin to cells was evaluated by MTT method (Beyotime Biotechnology). Briefly, RAW264.7 cells (2×10^5/ml) or EL4 cells (2×10^6/ml) were cultured in six replicates in 96-well plates in a volume of 200μl. Cells were incubated alone (control) or in presence of increasing concentrations of Con A or emodin (Sigma Chemical Co., St. Louis, MO, USA) for 24 h. Then the cells were incubated with a solution containing 0.5 mg MTT/mL phosphate-buffered saline at 37°C for 4 h. The MTT solution was removed and the cells were overlaid with 150 μL/well DMSO for 10 min at 37°C. The OD value was measured using a Bio-Rad microplate reader at 490 nm with DMSO as blank.

Western blot analysis

The liver tissues or cells were homogenized and centrifuged at 12,000 g for 10 min at 4 °C. The proteins were quantified by the Pierce BCA Protein Assay Kit (Thermo Fisher Scientific Inc., Rockford). Equivalent protein amounts (40 μg) were separated by 12% SDS-PAGE and transferred to polyvinylidene difluoride membranes (Millipore, Billerica, MA, USA), which were then blocked in TBST containing 5% defatted milk and incubated with primary antibodies specific for phosphorylated p38 MAPK (#4511, Cell Signaling Technology, USA), phosphorylated NF-κB p65 (#3036, Cell Signaling Technology, USA), total p38 MAPK (#9212, Cell Signaling Technology, USA), total NF-κB p65 (#ab7970, Abcam, USA), and β-actin (cytoplasmic protein marker, #4970, Cell Signaling Technology, USA) at 4 °C overnight. The membranes were then incubated with horseradish peroxidase- conjugated anti-rabbit or anti-mouse immunoglobulin G (Southern Biotechnology Associates, Inc., Birmingham, AL, USA). Bound antibodies were visualized by enhanced chemiluminescence (Thermo Fisher Scientific Inc., Rockford) and exposed to X-ray film. The changes in protein levels were normalized by the levels of β-actin proteins. The densitometric analysis was performed using Quantity One v4.62 (Bio-Rad, Inc., Berkeley, CA, USA).

Statistical analysis

All data were processed by the SPSS 16.0 software and presented as the mean ± SE. Analysis of variance (ANOVA) and LSD tests were used for comparisons among the groups and between the paired data, respectively. When the data were not normally distributed, the Mann-Whitney U test and the one-way non-parametric ANOVA (Kruskal-Wallis test) were used to compare quantitative variables between two groups and among more than two groups, respectively. A p value of less than 0.05 was considered to be statistically significant.

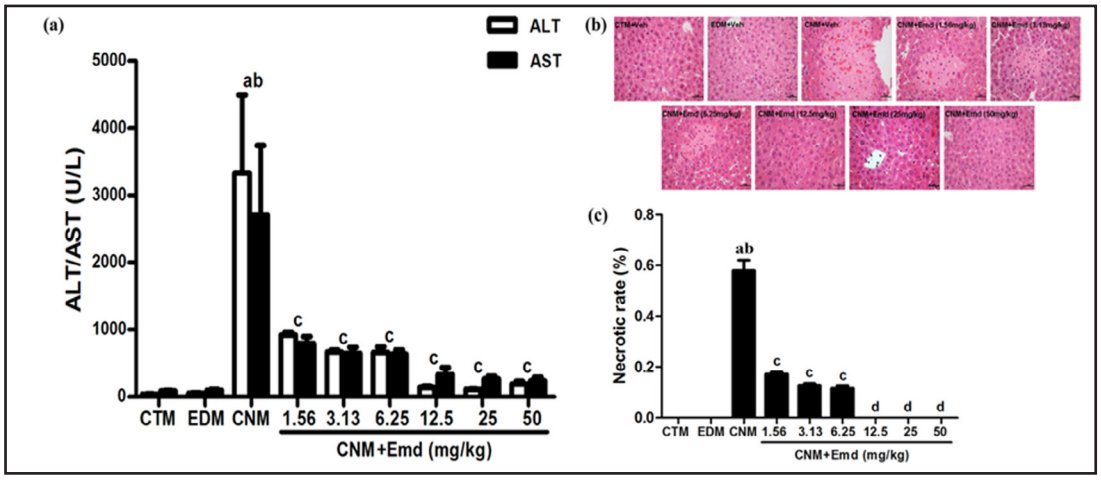

Fig. 1. Effects of different doses of emodin on hepatic injury in mice exposed to Con A. (a) Serum ALT and AST levels in control mice (CTM), emodin-administered mice (EDM), and Con A-induced mice (CNM) treated with vehicle (Veh) or emodin (Emd) at different doses. (b) Histological analysis of hepatic tissue. Representative images of liver sections from five mice are presented (H&E staining, original images 10×). (c) The area of necrosis was quantified for the HE-stained sections and is shown as percentage of liver area. [a]P <0.01, compared with normal control group; [b]P <0.01, compared with emodin group; [c]P <0.05, compared with Con A group; [d]P <0.01, compared with Con A group.

Results

Effects of different doses of emodin on hepatic injury in mice exposed to Con A

Increased serum ALT and AST levels (P <0.01) and confluent necrotic foci were observed at 10 h after exposure to Con A (Fig. 1). Fig. 1a shows that emodin administered 2 h before Con A at concentrations of 1.5625 mg/kg, 3.125 mg/kg, 6.25 mg/kg, 12.5 mg/kg, 25 mg/kg, and 50 mg/kg led to reduced serum ALT and AST levels in the mice (P <0.05 and P <0.01, respectively). However, small and scattered necro-inflammatory foci with polymorphonuclear cell infiltration were observed when emodin was administered at concentrations of 1.5625 mg/kg, 3.125 mg/kg, 6.25 mg/kg, while only sparse polymorphonuclear leukocyte infiltration and almost no necrotic foci were observed when emodin was given at concentrations of 12.5 mg/kg, 25 mg/kg and 50 mg/kg (Fig. 1b, c). However, there were no significant differences in serum ALT levels or AST levels when emodin was given at concentrations of 12.5 mg/kg, 25 mg/kg and 50 mg/kg.

Effects of emodin administered at different times on hepatic injury in Con A-exposed mice

Increased serum ALT and AST levels (P <0.01) and large areas of necrosis were observed at 10 h after Con A administration (Fig. 2), which could be reversed by emodin administered 2 h before the Con A challenge (P <0.01). However, Fig. 2 also demonstrates that emodin was not able to alleviate Con A-induced liver injury when given at 30 min, 60 min, 90 min, and 2 h after the Con A challenge (P>0.05).

Effects of emodin on mRNA levels of IFN-γ, TNF-α, IL-1β, IL-6, IL-12, and iNOS in livers of mice

Fig. 3 shows that the levels of hepatic IFN-γ, TNF-α, IL-1β, IL-6, IL-12, and inducible nitric oxide synthase (iNOS) mRNA in Con A-induced mice were significantly higher than those in the normal mice (P <0.01). However, emodin ingestion dose-dependently restored hepatic IFN-γ, TNF-α, IL-1β, IL-6, IL-12, and iNOS mRNA levels in Con A-induced mice (P <0.05 or P <0.01).

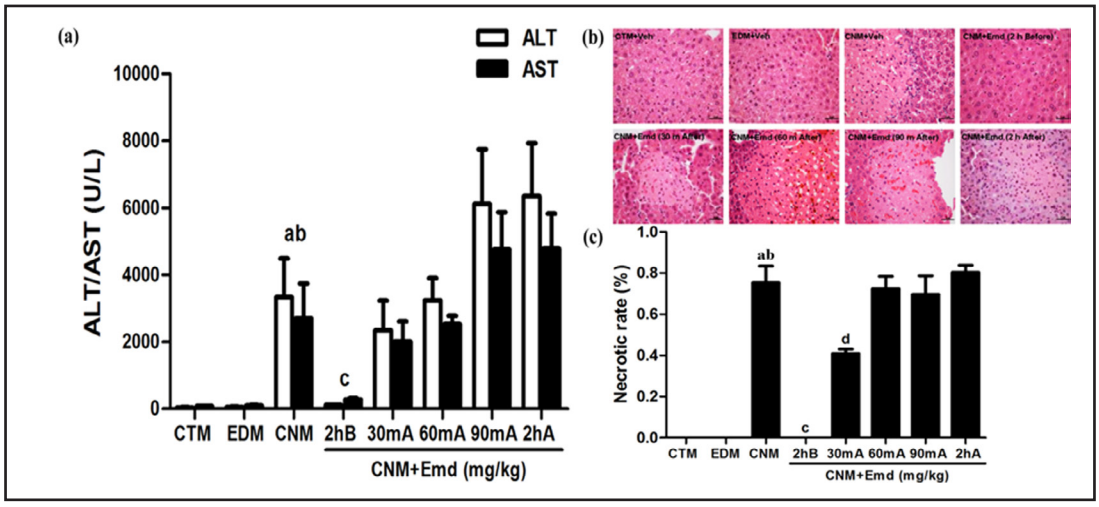

Fig. 2. Effects of emodin given at different time points on hepatic injury in mice exposed to Con A. (a) Serum ALT and AST levels in control mice (CTM), emodin-administered mice (EDM), and Con A-induced mice (CNM) treated with vehicle (Veh) or emodin (Emd, 25 mg/kg) at different time points. (b) Histological analysis of hepatic tissue. Representative images of liver sections from five mice are presented (H&E staining, original images 10×). (c) The area of necrosis was quantified for H&E-stained sections and is shown as percentage of liver area. [a]P <0.01, compared with normal control group; [b]P <0.01, compared with emodin group; [c]P <0.05, compared with Con A group; [d]P <0.01, compared with Con A group. 2hB, 2 h before Con A challenge; 30mA, 30 m after Con A challenge; 60mA, 60 m after Con A challenge; 90mA, 90 m after Con A challenge; 2hA, 2 h after Con A challenge.

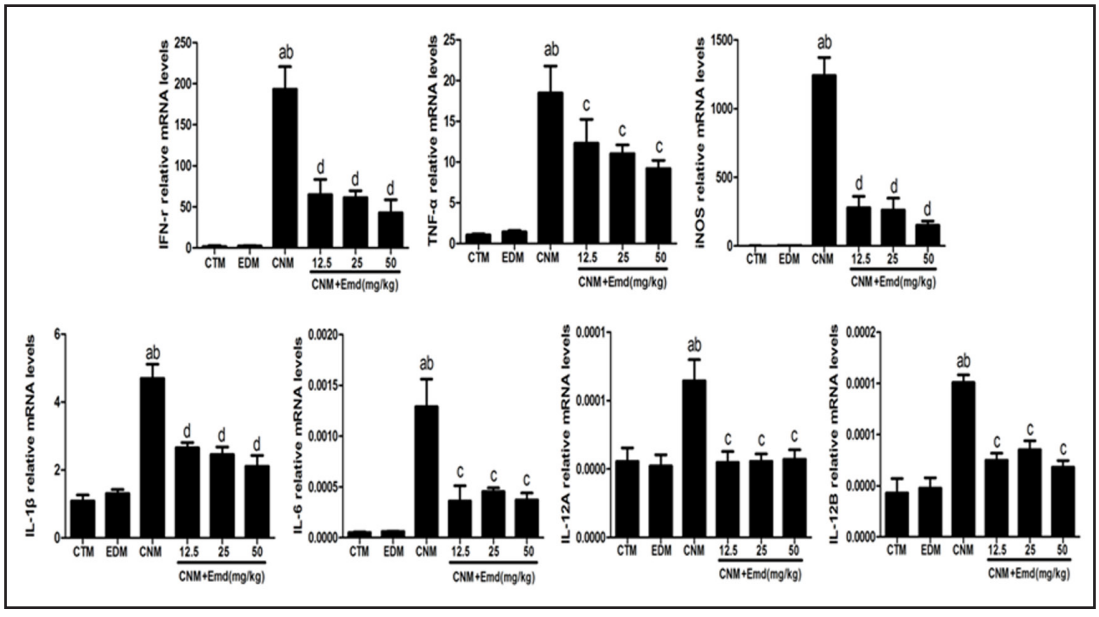

Fig. 3. Effects of emodin on mRNA levels of IFN-γ, TNF-α, IL-1β, IL-12, IL-6, and iNOS in livers of mice. [a]P <0.01, compared with normal control group; [b]P <0.01, compared with emodin group; [c]P <0.05, compared with Con A group; [d]P <0.01, compared with Con A group.

Effects of emodin on mRNA levels of ITGAM, CCL2, MIP-2 and its receptor, CXCR2, in livers of mice

As shown in Fig. 4, the Con A-induced mice showed higher mRNA levels of hepatic integrin alpha M (ITGAM), chemokine (CC motif) ligand 2 (CCL2), macrophage inflammatory protein 2 (MIP-2), and its receptor, chemokine (CXC motif) receptor 2 (CXCR2) compared

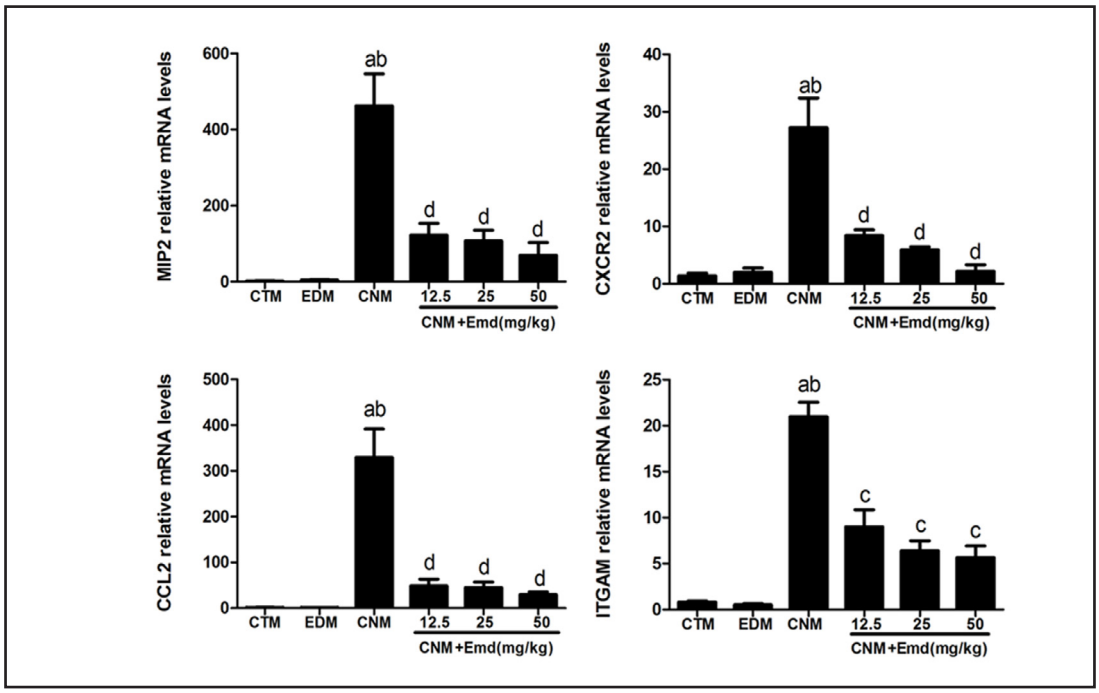

Fig. 4. Effects of emodin on mRNA levels of ITGAM, CCL2, MIP-2, and its receptor, CXCR2, in livers of mice. [a]P <0.01, compared with normal control group; [b]P <0.01, compared with emodin group; [c]P <0.05, compared with Con A group; [d]P <0.01, compared with Con A group.

with the normal mice (P <0.01). However, emodin administration dose-dependently restored hepatic ITGAM, CCL2, MIP-2 and CXCR2 mRNA levels in Con A-induced mice (P <0.05 or P <0.01).

Effects of emodin on p38 MAPK and NF-κB activation in livers of Con A-induced mice

To determine whether p38 MAPK and NF-κB are involved in the protective effects of emodin on liver impairment in Con A-induced mice, the hepatic p38 MAPK and NF-κB activity were examined. As shown in Fig. 5, although there were no significant differences in hepatic basic p38 MAPK and NF-κB protein levels in the control and Con A-induced groups, the hepatic phosphorylated levels of p38 MAPK and NF-κB were increased in Con A-induced mice (P <0.05 or P <0.01). However, emodin administration reversed the Con A- induced increase of hepatic phosphorylated p38 MAPK and NF-κB protein levels in the mice (P <0.05 or P <0.01).

Effects of emodin on CD4+ T cell and F4/80+ macrophage recruitment increased by Con A treatment

The effects of emodin on the infiltration of $CD4^+$ T cells and $F4/80^+$ macrophages in the livers of Con A-induced mice were determined by immunofluorescence. Fig. 6 shows that the numbers of $CD4^+$ T cells and $F4/80^+$ macrophages increased significantly in the livers after Con A injection (P <0.05 or P <0.01) but could be returned to basal levels following emodin treatment (P <0.05).

Effects of emodin on p38 MAPK and NF-κB activation in Con A-induced cells

As shown in Fig. 7, some toxicity was observed when Con A was given at 31.25 μg/ml in RAW264.7 cells, but no toxic effect were found in EL4 cells even when cells were exposed to Con A at 100 μg /ml. The viability of RAW264.7 cells and EL4 cells was not affected by 24 h incubation with emodin at concentrations of up to 12.5 μg/ml and 25 μg / ml, respectively (Fig. 7). Based on the results of MTT assay and a previous study [23], 15.63

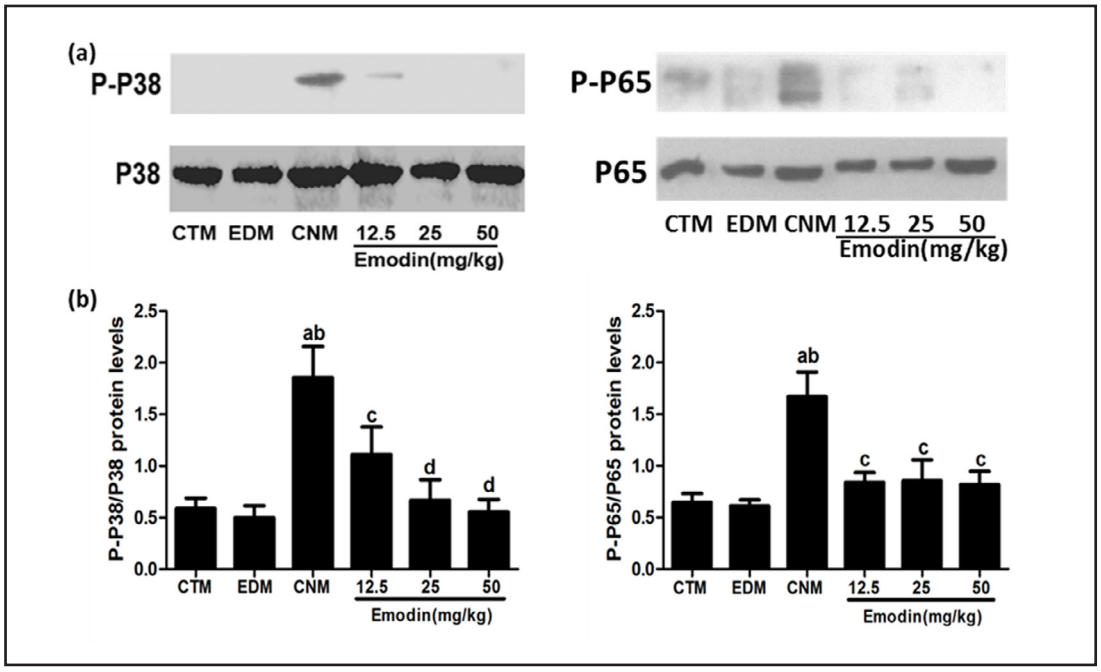

Fig. 5. Effects of emodin on p38 MAP kinase and NF-κB activation in livers of Con A-induced mice. (a) The phosphorylation and total p38 and NF-κB levels were determined using Western blotting. Representative images are shown for three independent experiments that showed similar results. (b) Band intensities for p38 and NF-κB phosphorylation were normalized by those for total p38 and NF-κB levels, respectively. [a]P <0.01, compared with normal control group; [b]P <0.01, compared with emodin group; [c]P <0.05, compared with Con A group; [d]P <0.01, compared with Con A group.

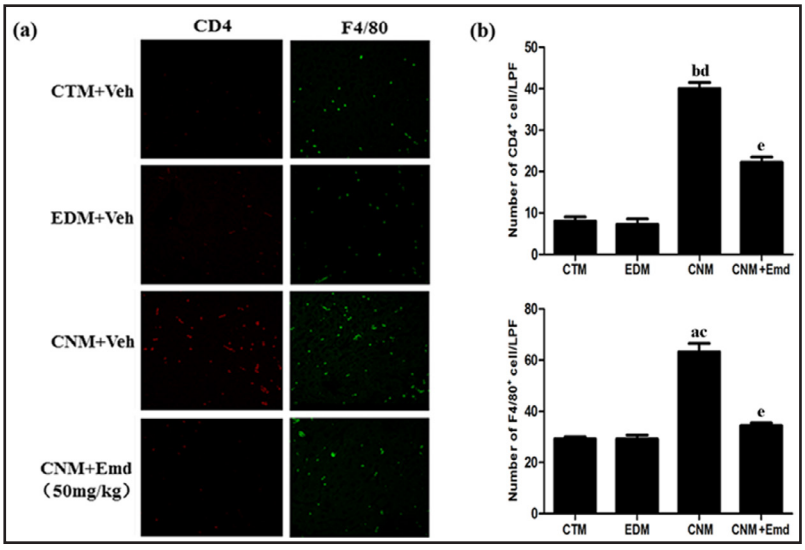

Fig. 6. Expression profiling of $CD4^+$ or $F4/80^+$ cells in livers of mice exposed to Con A. (a) Infiltration of $CD4^+$ T cells or of $F4/80^+$ macrophages in livers from mice exposed to Con A or from control mice were detected by immunofluorescence assays. (b) Quantifications of $CD4^+$ and $F4/80^+$ cells in livers of mice from each group. [a]P <0.05, compared with normal control group; [b]P <0.01, compared with normal control group; [c]P <0.05, compared with emodin group; [d]P <0.01, compared with emodin group; [e]P <0.05 compared with Con A group.

μg/ml and 4 μg/ml of Con A were used in RAW264.7 and EL4 cells, respectively; and emodin at concentrations of 12.5 μg/ml and 25 μg /ml were used in RAW264.7 and EL4 cells in our next study, respectively.

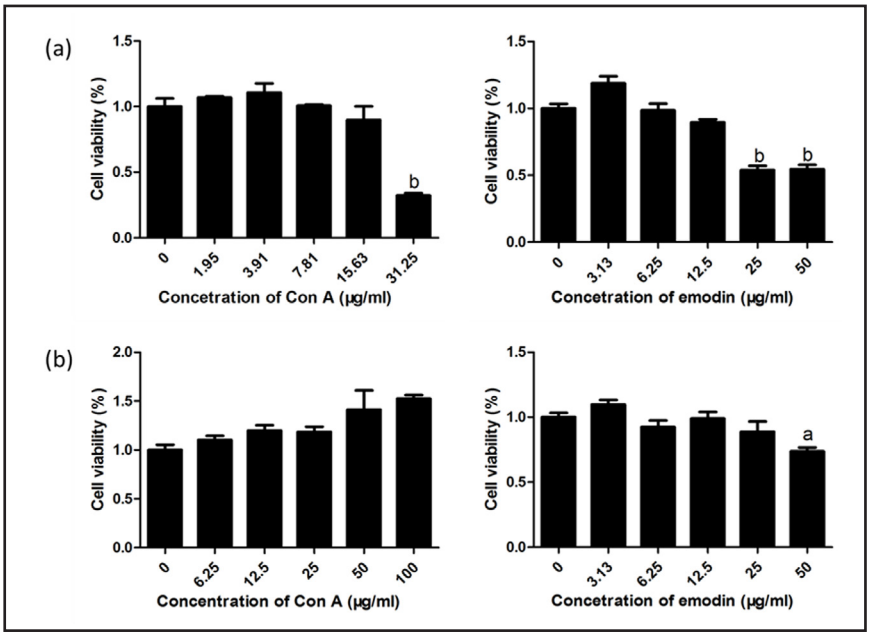

Fig. 7. Cytotoxicity of Con A and emodin on RAW264.7 and EL4 cells. (a) The cytotoxicity of Con A and emodin were determined in RAW264.7 cells using MTT assay. The representative result of three independent experiments is shown. (b) The cytotoxicity of Con A and emodin were determined in EL4 cells using MTT assay. The representative result of three independent experiments is shown. [a]P <0.05, compared with normal control group; [b]P <0.01, compared with normal control group.

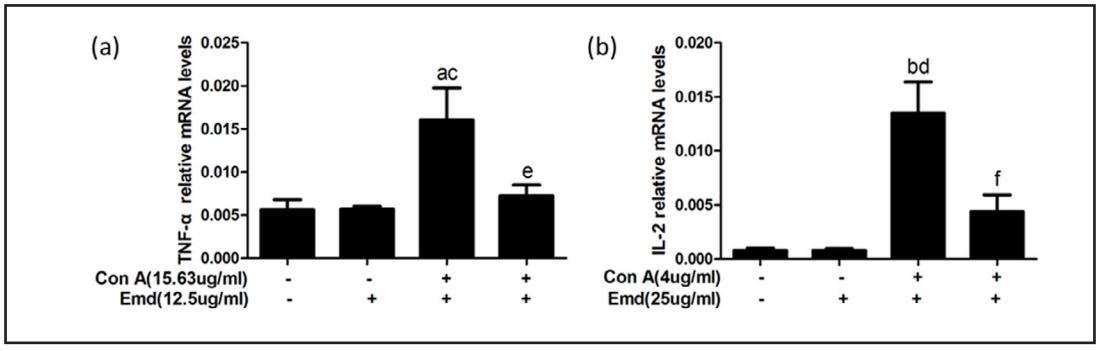

Fig. 8. Effects of emodin on mRNA levels of TNF-α and IL2 in cells. (a) The mRNA levels of TNF-α in RAW264.7 cells were determined using qRT-PCR. Representative images are shown for three independent experiments that showed similar results. (b) The mRNA levels of IL2 in EL4 cells were determined using qRT-PCR. Representative images are shown for three independent experiments that showed similar results. [a]P <0.05, compared with normal control group; [b]P <0.01, compared with normal control group; [c]P <0.05, compared with emodin group; [d]P <0.01, compared with emodin group; [e]P <0.05 compared with Con A group; [f]P <0.01 compared with Con A group.

Fig. 8 shows that the level of TNF-α induced by Con A in RAW 264.7 cells increased significantly, as compared with control group (P <0.01). Moreover, the level of TNF-α of Con A plus emodin group were obviously lower than those of Con A group (P <0.01). In Fig. 8, Con A-induced production of IL-2 in EL4 cells was significantly (P <0.01) suppressed by emodin. These *in vitro* results explained that emodin could reduce the inflammatory factors induced by Con A in RAW264.7 and EL4 cells.

Fig. 9 and 10 show that although there were no significant differences in unphosphorylated p38 MAPK and NF-κB protein levels in the control and Con A-induced groups, the phosphorylated levels of p38 MAPK and NF-κB were increased in Con A-induced cells (P <0.05 or P <0.01). However, emodin administration reversed the Con A- induced

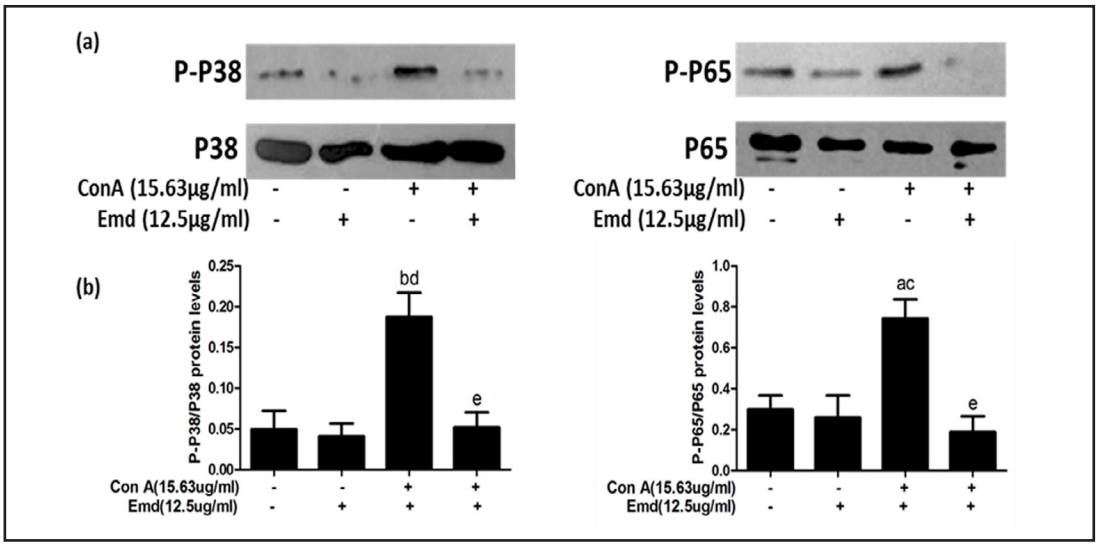

Fig. 9. Effects of emodin on p38 MAP kinase and NF-κB activation in RAW264.7 cells. (a) The phosphorylation and total p38 MAP kinase and NF-κB levels were determined using Western blotting. Representative images are shown for three independent experiments that showed similar results. (b) Band intensities for p38 MAP kinase and NF-κB phosphorylation were normalized by those for total p38 MAP kinase and NF-κB levels. [a]P <0.05, compared with normal control group; [b]P <0.01 compared with normal control group; [c]P <0.05 compared with emodin group; [d]P <0.01 compared with emodin group; [e]P <0.01 compared with Con A group.

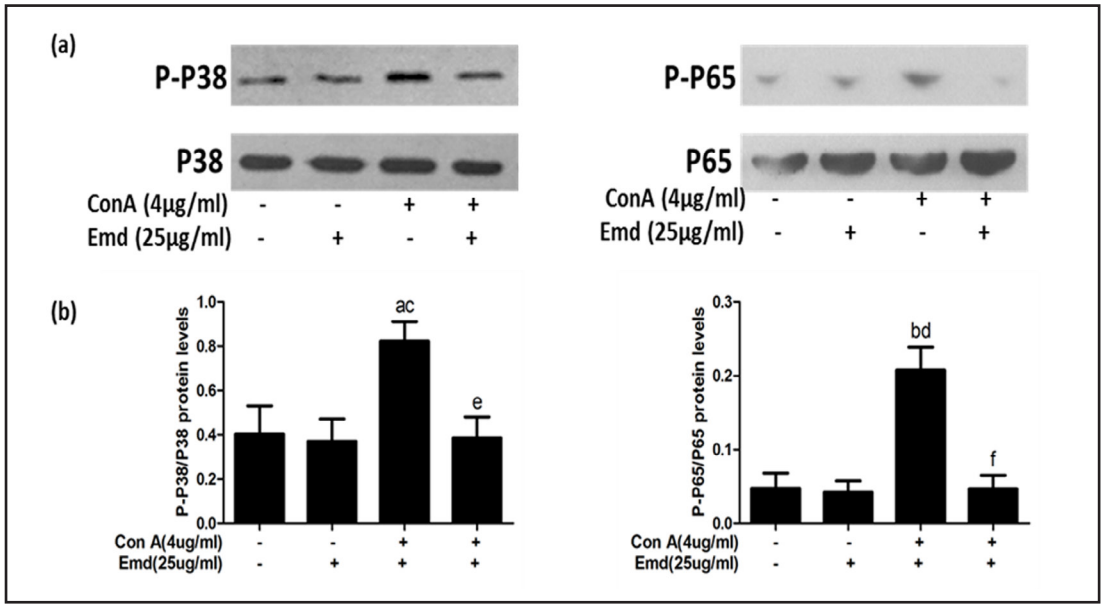

Fig. 10. Effects of emodin on p38 MAP kinase and NF-κB activation in EL4 cells. (a) The phosphorylation and total p38 MAP kinase and NF-κB levels were determined using Western blotting. Representative images are shown for three independent experiments that showed similar results. (b) Band intensities for p38 MAP kinase and NF-κB phosphorylation were normalized by those for total p38 MAP kinase and NF-κB levels. [a]P <0.05, compared with normal control group; [b]P <0.01 compared with normal control group; [c]P <0.05 compared with emodin group; [d]P <0.01 compared with emodin group; [e]P <0.05 compared with Con A group; [f]P <0.01 compared with Con A group.

increase in phosphorylated p38 MAPK and NF-κB protein levels in the two cells (P <0.05 or P <0.01).

Discussion

Emodin is the main effective component of rhubarb, and it has not been demonstrated to be associated with significant deleterious side effects. Dang SS et al. described the inhibitory effects of emodin in combination with astragalus polysaccharide on the replication of HBV *in vitro* [24]. However, little is known regarding the preventive role of emodin in fulminant hepatitis. In the present study, the mice with Con A- induced hepatitis showed high serum levels of ALT and AST concomitant with hepatic injury. However, treatment with emodin alone reduced the serum levels of ALT and AST and hepatic levels of IFN-γ, TNF-α, IL-1β, IL-6, IL-12, iNOS, ITGAM, CCL2, MIP-2 and CXCR2 and attenuated hepatic injury in the mice with Con A- induced hepatitis. Also, the results of our study demonstrated that the inhibition of these pro-inflammatory cytokines and chemokines may be associated with the suppression of the infiltration of $CD4^+$ T cells and macrophages as well as the activation of p38 MAPK-NF-κB signaling pathway in the two cells.

Many studies have shown that immunoregulatory cytokines play a central role in the pathogenesis of Con A-induced hepatitis, and previous studies have reported the pro-inflammatory roles of the cytokines TNF-α, IL-1β, IFN-γ, IL-12, and IL-6 [12-14, 25]. The up-regulation of pro-inflammatory cytokines, such as IFN-γ and TNF-α, by Con A injection was shown to directly induce hepatocellular apoptosis and necrosis [26, 27]. iNOS is mainly present in macrophages and hepatocytes and can be induced by TNF-α or IFN-γ in many types of immune cells [28, 29].

Chemokines are small heparin-binding proteins that direct the movement of circulating leukocytes to sites of inflammation or injury. Chemokines and their receptors are now known to play crucial roles in engendering the adaptive immune response and contributing to the pathogeneses of a variety of diseases [30]. ITGAM, which is also known as cluster of differentiation molecule 11B (CD11B), mediates the inflammatory response by regulating leukocyte adhesion and migration and has been implicated in several immune processes, such as phagocytosis, cell-mediated cytotoxicity, chemotaxis and cellular activation [31]. CCL2 is also referred to as monocyte chemotactic protein-1 (MCP-1). It recruits monocytes, memory T cells, and dendritic cells to sites of inflammation caused by tissue injury or infection [32, 33]. The murine CXC chemokine MIP-2 is a functional analog of human IL-8. Similar to IL-8, it acts as a potent neutrophil chemoattractant.

The current study revealed the overexpression of hepatic IFN-γ, TNF-α, IL-1β, IL-12, IL-6, and iNOS in Con A-induced mice. However, emodin ingestion decreased the expression of these cytokines, which paralleled improvements in serum ALT and AST levels and reduced hepatic injury. The increased production of ITGAM, CCL2, MIP-2, and its receptor, CXCR2, in the livers of Con A-induced mice was also found in the present study, which could be attenuated by emodin treatment. These observations indicate that emodin reduced serum ALT and AST overexpression and liver injury through its inhibition of hepatic pro-inflammatory cytokines and chemokines.

As an important member of the MAPK family, p38 MAPK is considered to be closely related to the regulation of inflammation, stress and apoptosis. Wang et al. analyzed the structures of emodin and the p38 MAPK protein using molecular designing software and found that some of the chemical groups of emodin bind to the dewatering groups of the p38 MAPK protein, suggesting the possibility that emodin directly binds to p38 MAPK and inhibits its activity [34]. The activated form of p38 has been associated with the activation of NF-κB [35-37]. Inactive NF-κB (mainly p65/p50 dimers) is sequestered in the cytoplasm. Once it becomes phosphorylated and activated, it translocated to the nucleus where it binds to the promoters of specific target genes and up-regulates the transcription of cytokines. NF-κB plays a central role in the regulation of diverse biological processes, including the immune response, development, cell growth and survival [38, 39]. Previous studies have shown that NF-κB regulates the release of inflammatory cytokines in Con A-induced hepatitis, and the blockade of NF-κB activation can reduce the expression of these cytokines [40, 41]. Thus, we hypothesized that emodin exerted its protective effects on Con A-induced hepatitis

by inhibiting the activation of the p38 MAPK-NF-κB signaling pathway. The current study revealed that the activation of p38 MAPK and NF-κB protein were augmented in the livers of mice and that emodin treatment significantly down-regulated these activations. These data suggest that the p38 MAPK-NF-κB pathway is involved in Con A-induced injury.

The recruitment of inflammatory cells to the liver by chemokines and the subsequent production of cytokines are the main factors for the pathogenesis and development of Con A-induced hepatitis, which is primarily characterized as T cell-mediated hepatic damage. Mounting evidence suggests that $CD4^+$ T cells are the predominant lymphocytes recruited to liver after the intravenous administration of Con A and that these cells play an important role in Con A-induced hepatitis because their depletion prevents liver damage following Con A injection [14]. Macrophages also play an important role in the induction of Con A-induced hepatitis, as confirmed by depletion treatment [42]. Thus, the suppressions of $CD4^+$ T lymphocytes and macrophage infiltration are therapeutic targets for Con A-induced hepatitis. In our study, the numbers of infiltrating $CD4^+$ T and $F4/80^+$ cells in the livers of the mice with Con A- induced hepatitis increased markedly but could be reduced by pretreatment with emodin. Also, *in vitro* studies showed that the activation of p38 MAPK and NF-κB protein were augmented in Con A-induced $CD4^+$ T cells and macrophages and that emodin treatment significantly down-regulated these activations. Therefore, $CD4^+$ T cells and macrophages are therapeutic targets of emodin that act in the pathogenesis of Con A-induced hepatitis in mice and are the main cells involved in p38 MAPK and NF-κB phosphorylation.

In summary, the present study first demonstrated that the targeting of emodin to the hepatic infiltration of $CD4^+$ T cells and macrophages and the activation of p38 MAPK-NF-κB pathway in the two cells prevented the Con A-induced elevation of ALT and AST levels and hepatic injury. The ability of emodin to inhibit activation of the p38 MAPK-NF-κB pathway resulted in the suppression of hepatic IFN-γ, TNF-α, IL-1β, IL-12, IL-6, iNOS, ITGAM, CCL2, and MIP-2, as well as the MIP-2 receptor, CXCR2. Emodin may have therapeutic applications in the prevention of fulminant hepatitis.

Acknowledgments

This work was supported by the State S&T Projects of 12th Five Year (2012ZX10002 007) and the Natural Science Foundation of China (81000730).

Disclosure Statement

The authors declare that they have no conflict of interest.

References

1 Ganem, D,Prince, AM: Hepatitis B virus infection--natural history and clinical consequences. N Engl J Med 2004;350:1118-1129.
2 Liaw, YF: Prevention and surveillance of hepatitis B virus-related hepatocellular carcinoma. Semin Liver Dis 2005;25:40-47.
3 Hoofnagle, JH, Doo, E, Liang, TJ, Fleischer, R, Lok, AS: Management of hepatitis B: summary of a clinical research workshop. Hepatology 2007;45:1056-1075.
4 Lok, AS,McMahon, BJ: Chronic hepatitis B. Hepatology 2007;45:507-539.
5 Belongia, EA, Costa, J, Gareen, IF, Grem, JL, Inadomi, JM, Kern, ER, McHugh, JA, Petersen, GM, Rein, MF, Sorrell, MF, Strader, DB, Trotter, HT: NIH consensus development statement on management of hepatitis B. NIH Consens State Sci Statements 2008;25:1-29.

6 Kruse, N, Neumann, K, Schrage, A, Derkow, K, Schott, E, Erben, U, Kuhl, A, Loddenkemper, C, Zeitz, M, Hamann, A, Klugewitz, K: Priming of CD4+ T cells by liver sinusoidal endothelial cells induces CD25low forkhead box protein 3- regulatory T cells suppressing autoimmune hepatitis. Hepatology 2009;50:1904-1913.
7 Lamontagne, L, Massicotte, E, Page, C: Mouse hepatitis viral infection induces an extrathymic differentiation of the specific intrahepatic alpha beta-TCR intermediate LFA-1 high T-cell population. Immunology 1997;90:402-411.
8 Jaruga, B, Hong, F, Sun, R, Radaeva, S, Gao, B: Crucial role of IL-4/STAT6 in T cell-mediated hepatitis: up-regulating eotaxins and IL-5 and recruiting leukocytes. J Immunol 2003;171:3233-3244.
9 Casini, A, Ricci, OE, Paoletti, F, Surrenti, C: Immune mechanisms for hepatic fibrogenesis. T-lymphocyte-mediated stimulation of fibroblast collagen production in chronic active hepatitis. Liver 1985;5:134-141.
10 Moebius, U, Manns, M, Hess, G, Kober, G, Meyer zum Buschenfelde, KH, Meuer, SC: T cell receptor gene rearrangements of T lymphocytes infiltrating the liver in chronic active hepatitis B and primary biliary cirrhosis (PBC): oligoclonality of PBC-derived T cell clones. Eur J Immunol 1990;20:889-896.
11 Zhang, H, Gong, Q, Li, JH, Kong, XL, Tian, L, Duan, LH, Tong, J, Song, FF, Fang, M, Zheng, F, Xiong, P, Tan, Z, Gong, FL: CpG ODN pretreatment attenuates concanavalin A-induced hepatitis in mice. Int Immunopharmacol 2010;10:79-85.
12 Hong, F, Jaruga, B, Kim, WH, Radaeva, S, El-Assal, ON, Tian, Z, Nguyen, VA, Gao, B: Opposing roles of STAT1 and STAT3 in T cell-mediated hepatitis: regulation by SOCS. J Clin Invest 2002;110:1503-1513.
13 Tu, CT, Han, B, Liu, HC, Zhang, SC: Curcumin protects mice against concanavalin A-induced hepatitis by inhibiting intrahepatic intercellular adhesion molecule-1 (ICAM-1) and CXCL10 expression. Mol Cell Biochem 2011;358:53-60.
14 Tiegs, G, Hentschel, J, Wendel, A: A T cell-dependent experimental liver injury in mice inducible by concanavalin A. J Clin Invest 1992; 90: 196-203.
15 Liu, LL, Gong, LK, Wang, H, Xiao, Y, Wu, XF, Zhang, YH, Xue, X, Qi, XM, Ren, J: Baicalin protects mouse from Concanavalin A-induced liver injury through inhibition of cytokine production and hepatocyte apoptosis. Liver Int 2007;27:582-591.
16 Li, HL, Chen, HL, Li, H, Zhang, KL, Chen, XY, Wang, XW, Kong, QY, Liu, J: Regulatory effects of emodin on NF-kappaB activation and inflammatory cytokine expression in RAW 264.7 macrophages. Int J Mol Med 2005;16:41-47.
17 Barnard, DL, Huffman, JH, Morris, JL, Wood, SG, Hughes, BG, Sidwell, RW: Evaluation of the antiviral activity of anthraquinones, anthrones and anthraquinone derivatives against human cytomegalovirus. Antiviral Res 1992;17:63-77.
18 Shieh, DE, Chen, YY, Yen, MH, Chiang, LC, Lin, CC: Emodin-induced apoptosis through p53-dependent pathway in human hepatoma cells. Life Sci 2004;74:2279-2290.
19 Hei, ZQ, Huang, HQ, Tan, HM, Liu, PQ, Zhao, LZ, Chen, SR, Huang, WG, Chen, FY, Guo, FF: Emodin inhibits dietary induced atherosclerosis by antioxidation and regulation of the sphingomyelin pathway in rabbits. Chin Med J (Engl) 2006;119:868-870.
20 Lee, W, Ku, SK, Kim, TH, Bae, JS: Emodin-6-O-beta-D-glucoside inhibits HMGB1-induced inflammatory responses in vitro and in vivo. Food Chem Toxicol 2013; 52: 97-104.
21 Meng, L, Yan, D, Xu, W, Ma, J, Chen, B, Feng, H: Emodin inhibits tumor necrosis factor-alpha-induced migration and inflammatory responses in rat aortic smooth muscle cells. Int J Mol Med 2012;29:999-1006.
22 Ding, Y, Zhao, L, Mei, H, Zhang, SL, Huang, ZH, Duan, YY, Ye, P: Exploration of Emodin to treat alpha-naphthylisothiocyanate-induced cholestatic hepatitis via anti-inflammatory pathway. Eur J Pharmacol 2008;590:377-386.
23 Kanwar, AS,Bhutani, KK: Effects of Chlorophytum arundinaceum, Asparagus adscendens and Asparagus racemosus on pro-inflammatory cytokine and corticosterone levels produced by stress. Phytother Res 2010;24:1562-1566.
24 Dang, SS, Jia, XL, Song, P, Cheng, YA, Zhang, X, Sun, MZ, Liu, EQ: Inhibitory effect of emodin and Astragalus polysaccharide on the replication of HBV. World J Gastroenterol 2009;15:5669-5673.
25 Verma, S,Thuluvath, PJ: Complementary and alternative medicine in hepatology: review of the evidence of efficacy. Clin Gastroenterol Hepatol 2007;5:408-416.

26 Tagawa, Y, Sekikawa, K, Iwakura, Y: Suppression of concanavalin A-induced hepatitis in IFN-gamma(-/-) mice, but not in TNF-alpha(-/-) mice: role for IFN-gamma in activating apoptosis of hepatocytes. J Immunol 1997;159:1418-1428.
27 Kano, A, Haruyama, T, Akaike, T, Watanabe, Y: IRF-1 is an essential mediator in IFN-gamma-induced cell cycle arrest and apoptosis of primary cultured hepatocytes. Biochem Biophys Res Commun 1999;257:672-677.
28 Geller, DA, Nussler, AK, Di Silvio, M, Lowenstein, CJ, Shapiro, RA, Wang, SC, Simmons, RL, Billiar, TR: Cytokines, endotoxin, and glucocorticoids regulate the expression of inducible nitric oxide synthase in hepatocytes. Proc Natl Acad Sci U S A 1993;90:522-526.
29 Kleinert, H, Schwarz, PM, Forstermann, U: Regulation of the expression of inducible nitric oxide synthase. Biol Chem 2003;384:1343-1364.
30 Charo, IF,Ransohoff, RM: The many roles of chemokines and chemokine receptors in inflammation. N Engl J Med 2006;354:610-621.
31 Solovjov, DA, Pluskota, E, Plow, EF: Distinct roles for the alpha and beta subunits in the functions of integrin alphaMbeta2. J Biol Chem 2005;280:1336-1345.
32 Xu, LL, Warren, MK, Rose, WL, Gong, W, Wang, JM: Human recombinant monocyte chemotactic protein and other C-C chemokines bind and induce directional migration of dendritic cells in vitro. J Leukoc Biol 1996;60:365-371.
33 Sun, LF, Shi, C, Yuan, L, Sun, Y, Yao, XX, Ma, JW, Huang, CM, Zhu, HF, Lei, P, Shen, GX: Expression of cytokines in mouse hepatitis B virus X gene-transfected model. J Huazhong Univ Sci Technolog Med Sci 2013;33:172-177.
34 Wang, J, Huang, H, Liu, P, Tang, F, Qin, J, Huang, W, Chen, F, Guo, F, Liu, W, Yang, B: Inhibition of phosphorylation of p38 MAPK involved in the protection of nephropathy by emodin in diabetic rats. Eur J Pharmacol 2006;553:297-303.
35 Saccani, S, Pantano, S, Natoli, G: p38-Dependent marking of inflammatory genes for increased NF-kappa B recruitment. Nat Immunol 2002;3:69-75.
36 Escors, D, Lopes, L, Lin, R, Hiscott, J, Akira, S, Davis, RJ, Collins, MK: Targeting dendritic cell signaling to regulate the response to immunization. Blood 2008;111:3050-3061.
37 Papachristou, DJ, Papadakou, E, Basdra, EK, Baltopoulos, P, Panagiotopoulos, E, Papavassiliou, AG: Involvement of the p38 MAPK-NF-kappaB signal transduction pathway and COX-2 in the pathobiology of meniscus degeneration in humans. Mol Med 2008;14:160-166.
38 Baeuerle, PA,Baltimore, D: NF-kappa B: ten years after. Cell 1996;87:13-20.
39 Bonizzi, G,Karin, M: The two NF-kappaB activation pathways and their role in innate and adaptive immunity. Trends Immunol 2004;25:280-288.
40 Feng, D, Mei, Y, Wang, Y, Zhang, B, Wang, C, Xu, L: Tetrandrine protects mice from concanavalin A-induced hepatitis through inhibiting NF-kappaB activation. Immunol Lett 2008;121:127-33.
41 Perkins, ND: Integrating cell-signalling pathways with NF-kappaB and IKK function. Nat Rev Mol Cell Biol 2007;8:49-62.
42 Higashimoto, M, Sakai, Y, Takamura, M, Usui, S, Nasti, A, Yoshida, K, Seki, A, Komura, T, Honda, M, Wada, T, Furuichi, K, Ochiya, T, Kaneko, S: Adipose tissue derived stromal stem cell therapy in murine ConA-derived hepatitis is dependent on myeloid-lineage and CD4+ T-cell suppression. Eur J Immunol 2013;43:2956-2968.